13.1

Electric arc synthesis of photoactive composite microparticles $ZnO/TiO_2/Nb_2O_5$

© M.Kh. Gadzhiev[1], F.F. Orudzhev[2], A.E. Muslimov[3]

[1] Joint Institute for High Temperatures, Russian Academy of Sciences, Moscow, Russia
[2] Dagestan State University, „Smart Materials"laboratory, Makhachkala, Russia
[3] Federal Research Center „Crystallography and Photonics", Russian Academy of Sciences, Moscow, Russia
E-mail: makhach@mail.ru

Received May 29, 2023
Revised July 8, 2023
Accepted July 9, 2023

The method of electric arc synthesis of photoactive multicomponent composite microparticles on the example of a $ZnO/TiO_2/Nb_2O_5$ system using a low-temperature plasma generator is proposed. Morphology and structural-phase composition of synthesized composite microparticles have been studied. Sold monstrated their record high photocatalytic activity (rate constant $128.6 \cdot 10^{-3}\,min^{-1}$) combined irradiation with ultraviolet and visible light

Keywords: titanium, zinc oxide, niobium, microparticles, photocatalysis, microscopy, morphology, structure.

DOI: 10.61011/TPL.2023.09.56708.19644

Studies into novel materials [1] and the production of heterogeneous systems based on well-proven TiO_2 [2] contribute to expanding the number of environmentally safe photocatalysts. Although TiO_2 is applied on an industrial scale, it has several key disadvantages: a narrow radiation absorption band, which falls within the ultraviolet range, and a low carrier mobility (high recombination rate). One way to raise the photosensitivity of TiO_2 in the visible range consists in forming composite metal/TiO_2 structures. The photoactivity of such systems increases due to charge transfer between a metal and TiO_2 [3]. Another method is the synthesis of nanocomposites [4–6] with a heterogeneous component based on materials with a narrower bandgap. Despite a slight bandgap width difference, heterogeneous systems based on ZnO and TiO_2 are regarded as fairly promising owing to the simplicity of formation of a heteroboundary and the similarity of band structures, which facilitates carrier transport across the boundary and contributes to a reduction in the probability of carrier recombination [7]. In addition, an end product (photocatalyst powder) with zinc oxide being dominant in its composition is significantly cheaper. It should be noted that current research is focused mostly on the synthesis of nanoscale systems, which, having a large surface fraction, offer exceptional versatility and performance. However, the synthesis of nanomaterials is a multistage process that requires extensive (up to 24 h) thermal treatment. In our view, the high-yield and energy-efficient method for synthesis of oxygen-containing catalyst powders with the use of thermal electric arc plasma is underappreciated. It appears that the technological difficulty of nanopowder synthesis hampers the widespread application of plasma processing techniques. That said, the photocatalytic efficiency of composite titanium-based microparticles synthesized by processing titanium micropowders in thermal electric arc plasma in the ambient atmosphere has already been demonstrated in our studies [8,9]. It was noted that the inner anode wall gets coated with a partially melted deposit in the course of extended processing of titanium micropowders; in addition, the profile of the gas-discharge channel of a plasmatron is altered. The use of zinc oxide (ZnO has a higher melting point) in a mixture with titanium may help suppress the side effect of melting of processed powders. The discussed synthesis technique is specific in that the composition of processed powders may be altered in multiple ways to achieve a synergistic effect (e.g., by adding niobium pentoxide inclusions to the photocatalyst [10]). The bandgap width, the similarity of surface chemistry of niobium pentoxide and titanium dioxide, and the proximity of ionic radii of Nb^{5+} and Ti^{4+} make it a perfect dopant that enhances the photoactivity of TiO_2.

In the present study, we consider the potential applications of electric arc plasma in synthesis of photoactive multicomponent composite $ZnO/TiO_2/Nb_2O_5$ microparticles and examine their morphology, structural and phase composition, and luminescent and photocatalytic properties.

A mixture of commercial high-purity zinc, titanium, and niobium powders was examined. The mass percentage of components was as follows: Zn — 85.5%, Ti — 11.6%, Nb — 2.9%. Microscopic studies were carried out using a JEOL (Japan) scanning electron microscope (SEM) fitted with an energy-dispersive X-ray (EDX) analysis. A Rigaku Miniflex 600 (Japan) diffractometer and CoK_a- radiation with a β-filter were used to record X-ray diffraction patterns. The MIS&S software was used to interpret these patterns. Photoluminescence spectra were recorded at a temperature of 300 K. A continuous-wave He–Cd- laser ($\lambda = 325$ nm) was the excitation source. The powder mixture was processed with thermal argon plasma in the anode region of

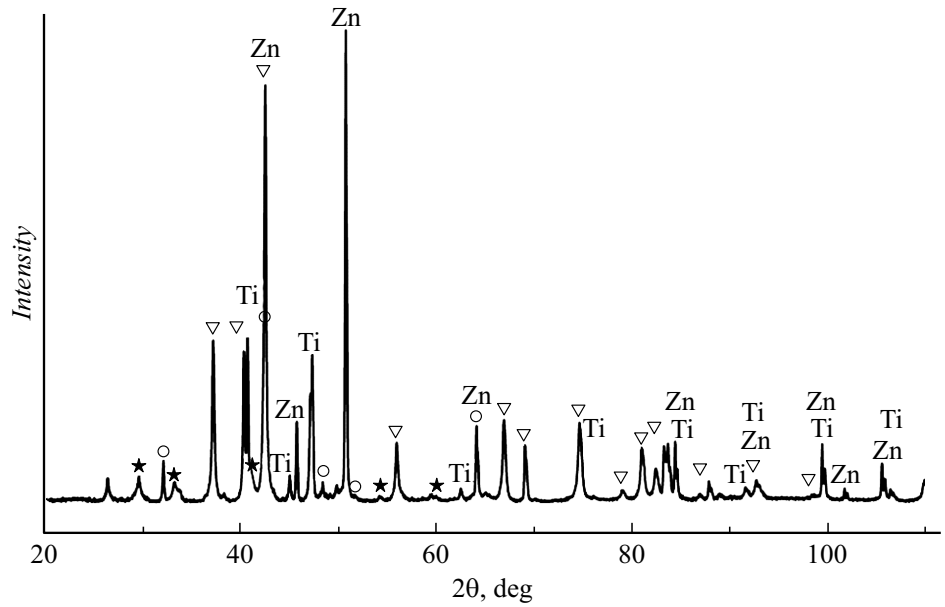

Figure 1. X-ray diffraction pattern of the synthesized composite $ZnO/TiO_2/Nb_2O_5$ photocatalyst. Triangles — ZnO, circles — TiO_2, and asterisks — Nb_2O_5.

a DC plasmatron with vortex stabilization and an expanding gas-discharge channel in the ambient atmosphere in accordance with the procedure outlined in [8]. the processing conditions were as follows: plasma-forming gas (argon) flow rate, 1.8 g/s; powder flow rate, 15 g/min; arc current, 150 A. The photocatalytic characteristics of samples were estimated by photodegradation of methylene blue (MB) in an aqueous solution (1 mg/l). Experiments were performed under irradiation with visible light (a 70 W Osram metal-halide lamp) and combined irradiation with ultraviolet and visible light (a 250 W Phillips high-pressure mercury lamp) without any cutoff light filters. A constant temperature of 26°C was maintained in the reaction vessel. Prior to irradiation, the reactor was kept in the dark until an adsorption-desorption equilibrium was established. Before the experiment, the suspension was subjected to ultrasonic treatment in a bath at 60 W and 40 kHz for 3 min (for photocatalyst degassing). The entire subsequent process was accompanied by mixing with a magnetic stirrer. A light source was located above the reactor at a distance of 10 cm. Sampling (5 ml) was performed in 15 min intervals. Particles were separated from the solution by centrifuging for 2 min with a PE-6926 (LLC „Ekroskhim") laboratory centrifuge. The MB concentration was measured using an SF-2000 spectrophotometer by the characteristic MB absorption peak at a wavelength of 663.7 nm. Following measurements, the solution was poured back into the reactor, and the process continued. The MB solution was also tested in similar conditions without the photocatalyst (photolysis) for comparison. The MB concentration was determined in accordance with the Beer–Lambert–Bouguer law.

What stands out is the fact that a partially melted deposit did not form on the exit nozzle of the plasmatron in the course of extended plasma processing of a mixture of metal powders (in earlier experiments with pure titanium microparticles, a deposit of this kind was observed). Owing to the specifics of growth of crystals with a wurtzite structure (predominant growth along [0001]), the process of oxidation of metallic zinc is more intense than the corresponding process for titanium: the oxide forms a loose deposit, which is easily penetrated by active oxygen that oxidizes deeper layers. The elemental composition determined using the EDX data (see the table) verifies the presence of oxide phases. According to X-ray diffraction data (Fig. 1), photocatalyst powder microparticles processed in plasma are composite structures containing both metallic and oxide phases: hexagonal Zn and Ti, hexagonal ZnO, rutile TiO_2, and monoclinic Nb_2O_5. SEM images (Fig. 2, *a*) revealed that composite microparticles processed in plasma have no definite shape and a size up to 200 μm with a „mossy" ZnO base and inclusions of various sizes, which contain titanium and niobium in both metal and oxide forms (Fig. 2, *b*). The mass percentage of zinc in the synthesized composite photocatalyst decreases (relative to the initial composition of the metal powder mixture). Loose zinc oxide is easily entrained by vortex flows to

Elemental composition of the photocatalyst powder according to EDX data

Element	Atomic fraction, %
O	48.73
Zn	38.34
Ti	11.33
Nb	1.60

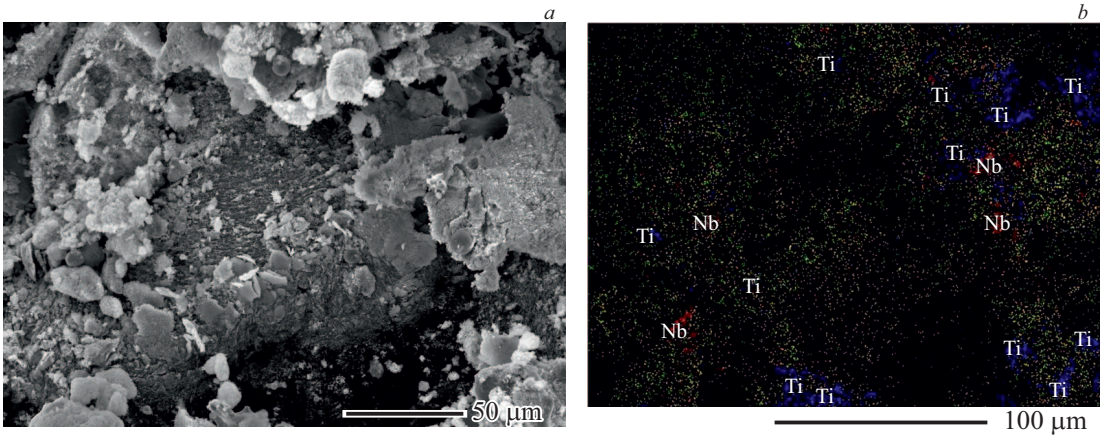

Figure 2. Electron microscope image (a) and EDX elemental map (b) for the composite $ZnO/TiO_2/Nb_2O_5$ photocatalyst. Zinc and oxygen are distributed uniformly over the entire microparticle surface.

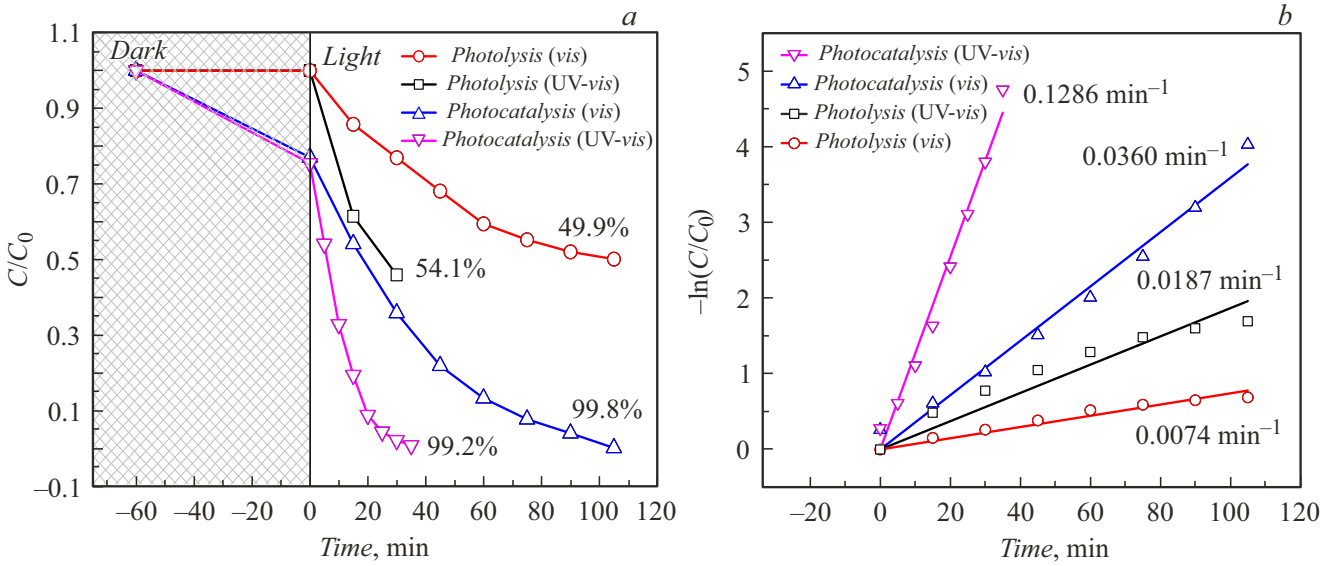

Figure 3. Curves of MB photodegradation under irradiation with ultraviolet and visible light and visible light only (a) and semi-logarithmic anamorphoses of kinetic curves of MB photodegradation (b) with the use of the composite $ZnO/TiO_2/Nb_2O_5$ photocatalyst.

the periphery of a plasma jet and enters the ambient environment. The photoluminescence spectrum consists of two bands: a narrow one with a maximum at 389 nm and a more intense broad band in the 400–550 nm region with a maximum at 415 nm. The narrow band corresponds to edge luminescence of ZnO [11]. The broad 400–550 nm band is a compound one and represents various luminescence centers in TiO_2 [12]. Also of note is the lack of a defect (green) ZnO luminescence band in the 550–700 nm region that is produced [13] by oxygen vacancies V_O or clusters consisting of V_O vacancies and interstitial zinc ions Zn_i.

The obtained materials were tested as photocatalysts in the process of destruction of a dye (methylene blue) under combined irradiation with ultraviolet and visible light. The results are shown in Fig. 3. The MB concentration decreased by approximately 25% in 60 min of testing performed after a preparatory dark stage that was needed to reach an adsorption-desorption equilibrium. These data are indicative of a strong adsorption capacity of the material with respect to MB. The dye decomposed almost completely (99.2%) in 35 min of irradiation with ultraviolet and visible light. The degree of decomposition attained within the same time interval without the catalyst was only 54.1%. The MB photodegradation rate constant was determined from the slope of linearized kinetic curves $\ln(C/C_0) - t$ with the use of the Langmuir–Hinshelwood model [14]. It can be seen (Fig. 3, b) that the reaction rate under combined irradiation with ultraviolet and visible light in the presence of the photocatalyst is 6.9 times higher than the photolysis rate. A high MB photodegradation rate was achieved: the rate constant was $128.6 \cdot 10^{-3}$ min^{-1}. A total of 99.8% of MB

decomposed in 105 min under irradiation with visible light, while only 49.9% of the dye decomposed within the same time interval without a catalyst. The reaction rate increased by a factor of 4.9 relative to the corresponding rate in the process of photolysis.

Thus, it was demonstrated that the obtained composite micropowder, which is composed mostly of semiconductors with a bandgap width of 3.0–3.4 eV [15], exhibits high photocatalytic activity in visible light and near-record activity levels under combined irradiation with ultraviolet and visible light. The enhancement of photocatalytic activity in nanoscale ZnO/TiO_2 [16] and TiO_2/Nb_2O_5 [17] composites has already been reported. An important finding made in the present study is that microscale (up to 200 μm in size) $ZnO/TiO_2/Nb_2O_5$ particles, which have a significant advantage in the ease of synthesis, also provide high reaction rates. Further studies of the structure of the composite material are needed to determined the mechanism of enhancement of the photocatalytic activity.

A method for electric arc synthesis of photoactive multicomponent composite $ZnO/TiO_2/Nb_2O_5$ microparticles with the use of a low-temperature plasma generator was proposed. It was found in the course of experiments that the introduction of zinc into the initial mixture provides an opportunity to extend the plasma processing time without risking the formation of partially melted deposits and nozzle clogging. The observed effect is attributable to the specific feature of oxidation of zinc powders (predominant growth of crystals with a wurtzite structure along [0001]). The morphology and the structural and phase composition of synthesized composite microparticles were examined. Their high photocatalytic activity (with a rate constant of $128.6 \cdot 10^{-3}\,\mathrm{min}^{-1}$) under combined irradiation with ultraviolet and visible light was demonstrated.

Funding

This study was carried out under state assignments of the Joint Institute for High Temperatures of the Russian Academy of Sciences (the work on synthesis of samples) and FSRC „Crystallography and Photonics“ of the Russian Academy of Sciences (examination of properties of samples).

Conflict of interest

The authors declare that they have no conflict of interest.

References

[1] Y. Chen, J. Cai, P. Li, G. Zhao, G. Wang, Y. Jiang, W. Sun, Nano Lett., **20** (9), 6807 (2020). DOI: 10.1021/acs.nanolett.0c02782
[2] J. Jeon, D.H. Kweon, B.J. Jang, M.J. Ju, J. Baek, Adv. Sustain. Syst., **4** (12), 2000197 (2020). DOI: 10.1002/adsu.202000197
[3] F.F. Orudzhev, A.B. Isaev, N.S. Shabanov, F.G. Gasanova, A.K. Idrisova, D.P. Babaeva, Int. J. Electrochem. Sci., **13**, 4548 (2018). DOI: 10.20964/2018.05.08
[4] J. Wu, C.E. Li, X.T. Chen, J. Zhang, L.L. Zhao, T.F. Huang, T. Hua, C. Zhang, B. Ni, X. Zhou, P.K. Liang, W.B. Zhang, J. Ind. Eng. Chem., **46**, 416 (2017). DOI: 10.1016/j.jiec.2016.11.012 24
[5] X. Chen, J. Zhang, X.D. Jiang, H.B. Wang, Z. Kong, J.H. Xi, Z.G. Ji, Mater. Lett., **229**, 277 (2018). DOI: 10.1016/j.matlet. 2018.07.051
[6] Z.F. Duan, Y. Zhu, Z.D. Hu, J.Y. Zhang, D.J. Liu, X. Luo, M.H. Gao, L. Lei, X.H. Wang, G.Y. Zhao, Ceram. Int., **46** (17), 27080 (2020). DOI: 10.1016/j.ceramint.2020.07.185
[7] Y.Z. Wang, S.P. Zhu, X.R. Chen, Y.G. Tang, Y.F. Jiang, Z.G. Peng, H.Y. Wang, Appl. Surf. Sci., **307**, 263 (2014). DOI: 10. 1016/j.apsusc.2014.04.023
[8] M.Kh. Gadzhiev, F.F. Orudzhev, A.E. Muslimov, M.V. Ilyichev, Tech. Phys. Lett., **49** (4), 1 (2023). DOI: 10.21883/PJTF.2023.07.54912.19321 [M.Kh. Gadzhiev, F.F. Orudzhev, A.E. Muslimov, M.V. Ilyichev, Tech. Phys. Lett., **49** (4), 1 (2023).].
[9] D.I. Yusupov, M.Kh. Gadzhiev, A.S. Tyuftyaev, V.F. Chinnov, M.A. Sargsyan, J. Phys.: Conf. Ser., **946**, 012176 (2018). DOI: 10.1088/1742-6596/946/1/012176
[10] C.L. Ücker, F. Riemke, V. Goetzke, M.L. Moreira, C.W. Raubach, E. Longo, S. Cava, Chem. Phys. Impact, **4**, 100079 (2022). DOI: 10.1016/j.chphi.2022.100079
[11] R. Raji, K.G. Gopchandran, J. Sci.: Adv. Mater. Dev., **2** (1), 51 (2017). DOI: 10.1016/j.jsamd.2017.02.002
[12] A. Saha, A. Moya, A. Kahnt, D. Iglesias, S. Marchesan, R. Wannemacher, D.M. Guldi, Nanoscale, **9** (23), 7911 (2017). DOI: 10.1039/c7nr00759k
[13] B.K. Meyer, H. Alves, D.M. Hofmann, W. Kriegseis, D. Forster, F. Bertram, J. Christen, A. Hoffmann, M. Straßurg, M. Dworzak, U. Haboeck, A.V. Rodina, Phys. Status Solidi B, **241** (2), 231 (2004). DOI: 10.1002/pssb.200301962
[14] A.V. Agafonov, A.A. Redozubov, V.V. Kozik, A.S. Kraev, Russ. J. Inorg. Chem., **60** (8), 906 (2015). DOI: 10.7868/S0044457X15080024 [A.V. Agafonov, A.A. Redozubov, V.V. Kozik, A.S. Kraev, Russ. J. Inorg. Chem., **60** (8), 906 (2015). DOI: 10.1134/s0036023615080021].
[15] P.L. Provenzano, G.R. Jindal, J.R. Sweet, W.B. White, J. Lumin., **92** (4), 297 (2001). DOI: 10.1016/s0022-2313(00)00264-7
[16] C. Cheng, A. Amini, C. Zhu, Z. Xu, H. Song, N. Wang, Sci. Rep., **4**, 4181 (2014). DOI: 10.1038/srep04181
[17] K.A. Michalow, D. Flak, A. Heel, M. Parlinska-Wojtan, M. Rekas, T. Graule, Environ. Sci. Poll. Res., **19** (9), 3696 (2012). DOI: 10.1007/s11356-012-0953-6

Translated by Ego Translating